WPMST1-PR(18) 20960

G. Tardini et al.

Detection of NBI-D acceleration by 2nd harmonic ICRF in ASDEX Upgrade via neutron spectrometry

Preprint of Paper to be submitted for publication in
Nuclear Fusion

This work has been carried out within the framework of the EUROfusion Consortium and has received funding from the Euratom research and training programme 2014-2018 under grant agreement No 633053. The views and opinions expressed herein do not necessarily reflect those of the European Commission.

Detection of NBI-D acceleration by 2nd harmonic ICRF in ASDEX Upgrade via neutron spectrometry

G. Tardini‡, R. Bilato, R. Fischer, M. Weiland, and the ASDEX Upgrade Team

Max-Planck-Institut für Plasmaphysik, EURATOM Association, Boltzmannstraße 2,
85748 Garching, Germany

Abstract. Second harmonic absorption of radio frequency in the Ion Cyclotron Range of Frequency (ICRF) by fast D is expected in the case of H minority heating at the fundamental cyclotron frequency, provided the ion Larmor radius is of the order of the RF-wavelength, as it is for Neutral Beam Injection (NBI)-D ions. In tokamaks a strong increase of neutron production is observed when such an ICRF heating is applied on top of NBI, often referred to as "synergy effect".

On ASDEX Upgrade a scintillator-based Compact Neutron Spectrometer (CNS) is available outside the torus hall, with perpendicular view through the plasma equatorial plane, measuring Pulse Height Spectra (PHS), which allow to infer the ion distribution functions, in particular the suprathermal tail.

The measured PHS exhibit clear energetic tails when ICRF is applied in the presence of NBI, proving there's an overproportional tail in the fast-ion distribution at the high energy end. The PHS in the CNS line-of-sight are modelled coupling kinetic

---

‡ Corresponding author: git@ipp.mpg.de

solvers with wave codes. Unfolding the PHS into neutron emission spectra allows to quantify the maximum fast ion energy with significant occurrence, showing a non-negligible population around 500 keV, significantly higher than the NBI energy. A sensitivity study assesses the maximum fast ion energy compatible with the measured PHS, confirming the presence of 500 keV D ions.

Keywords: Neutron spectrometry, scintillator, pulse height spectrum, ICRF, kick operator

1. Introduction

A typical heating scheme for tokamak D plasmas with Radio-Frequency (RF) waves is based on the excitation of the fast-wave in the Ion Cyclotron Range of Frequencies (ICRF) for the H minority at the fundamental cyclotron frequency. In presence of high T_i or significant suprathermal D population, there is a finite absorption by D (majority) at the 2nd harmonic, which is a Finite Larmor Radius (FLR) effect, if the ion Larmor radius is comparable to the RF wavelength. In the case of NBI heated plasmas, this effect is expected to be significant, because the ion Larmor radius scales like $\sqrt{E_D}$, E_D being the D-ion energy. Anomalously high neutron production rate was so far the main experimental evidence for ICRF D acceleration at higher harmonics [1] [2].

A comprehensive set of fast ions diagnostics in ASDEX Upgrade allows now a direct measurement of the suprathermal D population [3]. The Neutron Emission Spectrum (NES) contains information on the fast ions distribution function, because fusion neutrons are Doppler shifted depending on the velocities of the reacting deuterons. On ASDEX Upgrade a Compact Neutron Spectrometer (CNS) is available, based on the liquid organic scintillator BC501a (former NE213) [4] [5]. A photo-multiplier collects and amplifies the scintillation signal which is then digitalised with a Digital Acquisition system [6] and then processed to discriminate gamma from neutron events. The detector collects the light produced by recoil protons. Since a proton can receive any energy between zero and the incoming neutron energy in the elastic scattering process, and the detector response is energy dependent, the NES are convoluted with the detector response function: the directly measured quantity is, in fact, the Pulse Height Spectrum (PHS). Details about the detector, the acquisition board and the discrimination algorithm can be found in [4].

2. "Anomalous" increase of the neutron rate

As observed in the past, adding ICRF heating with H-minority absorption at the fundamental frequency in the plasma core in a NBI-heated plasma produces a strong increase of the neutron rate (see Fig. 1). The neutron rate, before and after switching on the ICRF, is measured with two completely independent detectors, based on different principles: a fission chamber (FIS2) placed in a moderator in the torus hall next to the tokamak (orange trace in Fig. 1); the CNS located outside the torus hall (blue trace). The uncalibrated signals are rescaled to show the accurate agreement of the

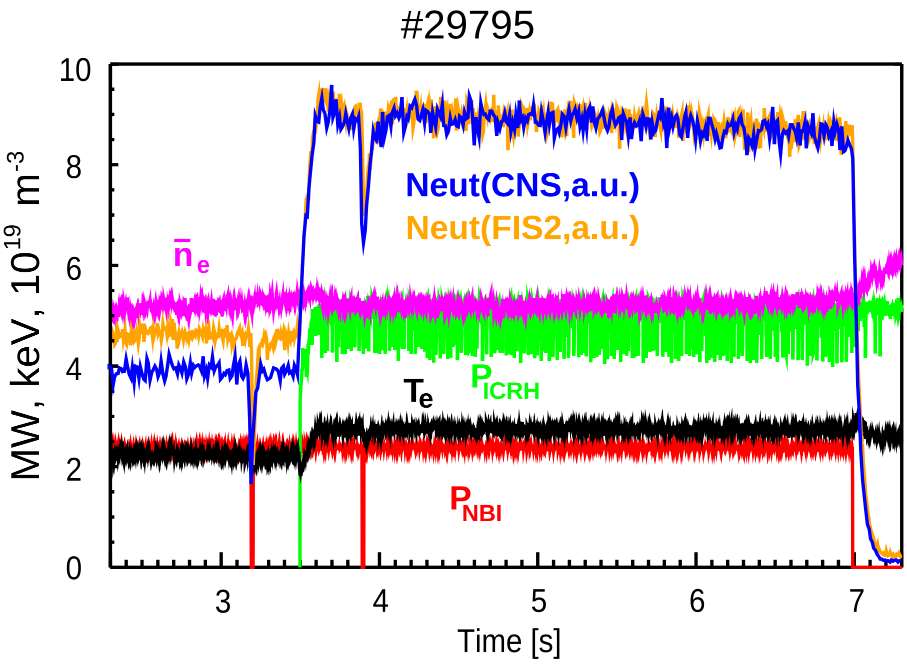

Figure 1. Time traces for discharge # 29795

ratio between the neutron rate with ($= y_{NBI+IC}$) and without ICRF ($= y_{NBI}$). Both diagnostic systems measure an increase of the neutron rate by factors 1.5-3 when ICRF is switched on, for all analysed discharges (see blue and orange symbols in Fig. 7). As Fig. 2 shows, this cannot be simply explained with the observed change in the kinetic profile, by modifying only the slowing down time. If no interaction of the wave with the suprathermal D population is assumed, the increase of the neutron rate simulated with the TRANSP code is not significant, when ICRF is added at 3.5 s. Precisely, the increase is roughly a factor 2 in the experiment (Fig. 1) while it's only 1.1 in the simulation.

Note that for the modelled neutron production we can distinguish between thermonuclear, beam-beam and beam-target neutrons. Since beam-targer reactions are dominant in the discharges analysed in this work (see red trace in Fig. 2), as already observed in ASDEX Upgrade NBI heated plasmas [7], the NES provides useful information for the fast ion energy distribution.

The "anomalous" increase in neutron rate is a very robust and reproducible observation. It has been explained as direct absorption of RF waves by D-ions with a large Larmor radius, such as fast NBI-D ions [1]. This explanation seems confirmed by recent measurements with the Fast Ion D-Alpha (FIDA) diagnostics [3]. However, FIDA cannot measure accurately fast ions above energies of ~ 150 keV, due to the charge exchange cross-section having a maximum around 60 keV, thus reducing the signal-to-noise ratio at high energies [3]. Moreover, such an increase of the neutron

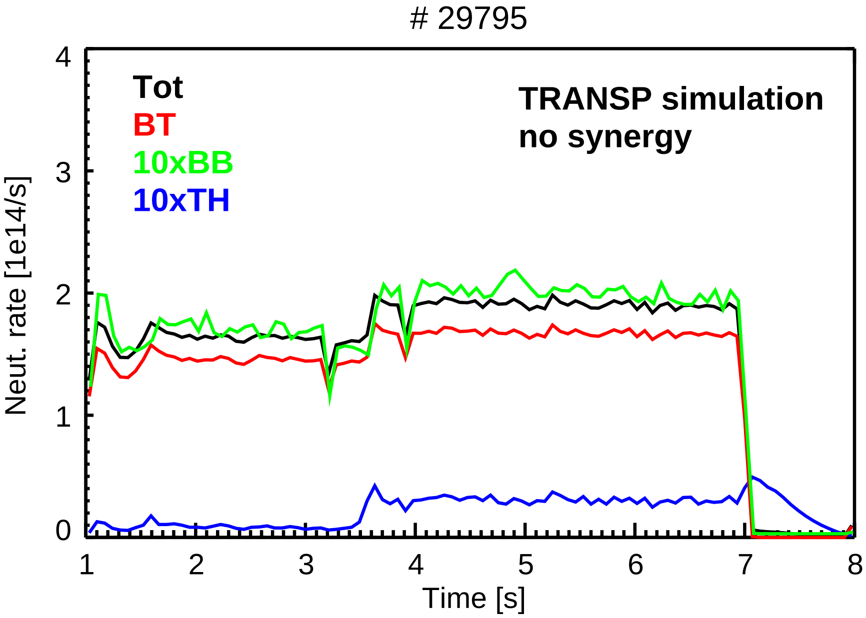

Figure 2. Neutron rate for discharge # 29795, simulated without any synergy model: total signal (black), beam-target (red), 10x thermonuclear (blue), 10x beam-beam (green). Beam-target reactions are 90% of the total yield.

rate could be explained also with a lesser sensitivity of NBI-D ions to turbulence or in general to a reduction of turbulent transport in presence of fast ions [9].

3. Energetic tails in Pulse Height Spectra and Neutron Emission Spectra

The CNS measures PHS, which corresponds roughly to the energy distribution of the recoil protons in the scintillator cellafter the scattering with the incoming neutrons. A PHS is the convolution of the NES with the instrumental response functions [8]. In Fig. 3 we compare the PHS in the phase with NBI only (red) with the one in the NBI+ICRF phase (green line).

The PHS is unfolded into a NES, which contains informatoin on the fast ion

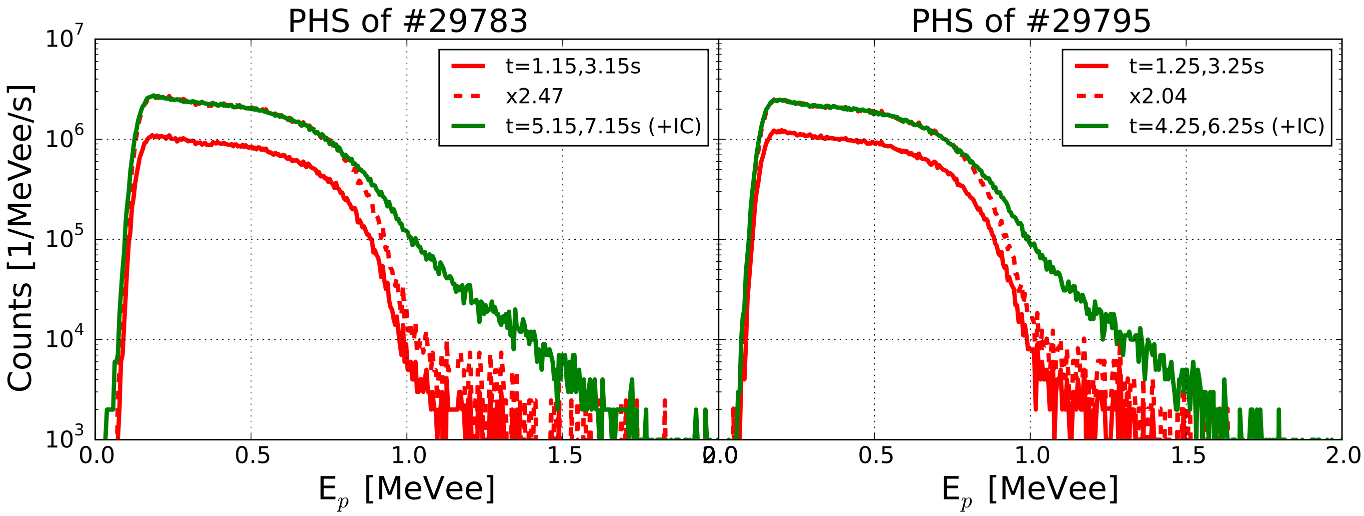

Figure 3. Semilogarithmic plot of the PHS for discharges #29783 and #29795 and. NBI+ICRF phase (green) and NBI only phase (red): actual count (continuous) and rescaled (dashed).

distribution. The deconvolution is performed using two codes, both based on the maximum entropy Ansatz: the MAXED code [10] and the Deconvolution method with Adaptive Kernel (DAK) [11]. In Fig. 4 both unfolding methods show qualitiatively and quantitatively similar NES. The characteristic double peak feature associated with a perpendicular cone-of-sight is clearly visible. The energetic tail is significant, the maximum neutron energy moves from ~ 3 to ~ 4 MeV when ICRF is added, proving that ions are accelerated beyond the NBI energy. A few artifacts are present at both the low and the high energy tail, with both unfolding methods, due to the slightly hollow instrumental response [8]. Howevever, we can have an approximate estimate of the maximum fast ion energy by using the simple formula $\Delta E_n \approx \sqrt{E_{fus} E_{fi,max}}$, ΔE_n being $E_{max} - E_{fus}$. Substituting $E_{fus} = 2.45$ MeV and $E_{fi,max} = 60$ keV, one obtains

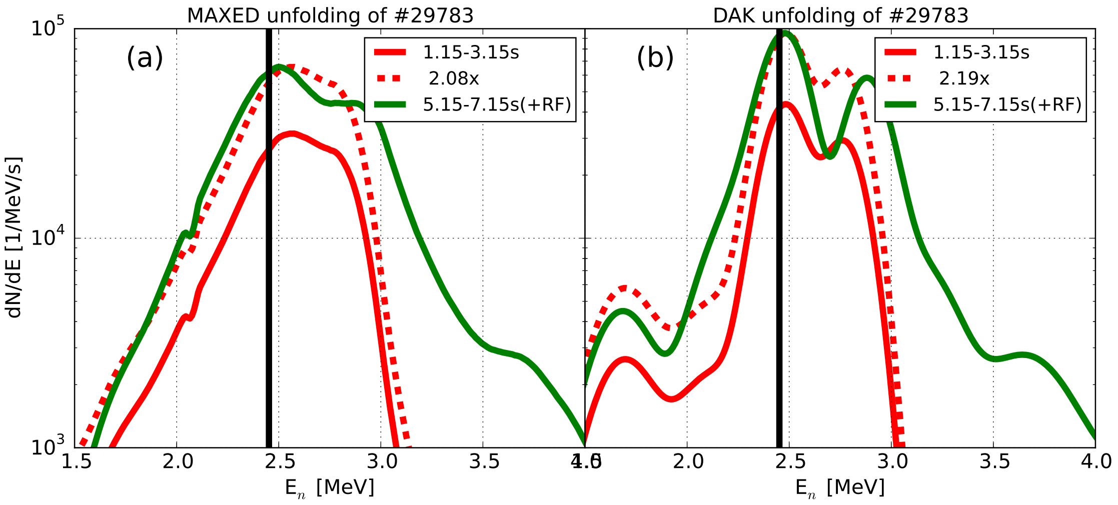

Figure 4. Semilogarithmic plot of the NES for discharge#29783, unfolding the experimental PHS with the MAXED code. NBI+ICRF (green) and NBI only phase (red): original (continuous) and rescaled (dashed). Unfolding with the (a) MAXED and (b) DAK codes.

$\Delta E_n \approx 0.4$ MeV, consistent with the red distribution in Fig. 4. A $\Delta E_n \approx 1.2$ MeV, observed in the green curves of Fig. 4 (a) and (b) corresponds to $E_{fi,max} \approx 500$ keV.

4. Modelling the NBI-ICRF synergy

The synergy effect between ICRF waves and a NBI-generated fast ion population has been recently modelled with different approaches. A quasi-linear RF-kick operator accounts for D acceleration in the MonteCarlo ansatz of TRANSP/NUBEAM [12], with a net momentum-trasfer to fast ions when they transit through the resonant region of the RF-field. The alternative approach is based on the TORIC+SSFPQL package [1]. TRANSP, on the one hand, follows the fast-ion orbits with a realistic collision operator, thus predicting fast ion losses and the slowing down process accurately and time-dependent. The TORIC+SSFPQL suite, on the other hand, has a consistent treatment of the back-reaction of the ICRF-NBI deformed distribution function onto wave-propagation and absorption.

According to both code packages, fast D-ions are accelerated well beyond the NB injection energy of 60 keV, as shown in Fig. 5 (c) for the TRANSP/NUBEAM simulatoin with RF-kick operator. In Fig. 5 (b) the same time point t=6.25 s (with NBI and ICRF) is simulated without RF-kick operator: obviously there is no significant fraction of fast ions above the injection energy. Fig. 5 (a) has a rather similar distribution as (b), being the simulation at 2.15 s, when there is no ICRF applied yet. Even if the phase-space density of fast ions beyond 60 keV, as predicted including the RF-kick, Fig. 5 (c),

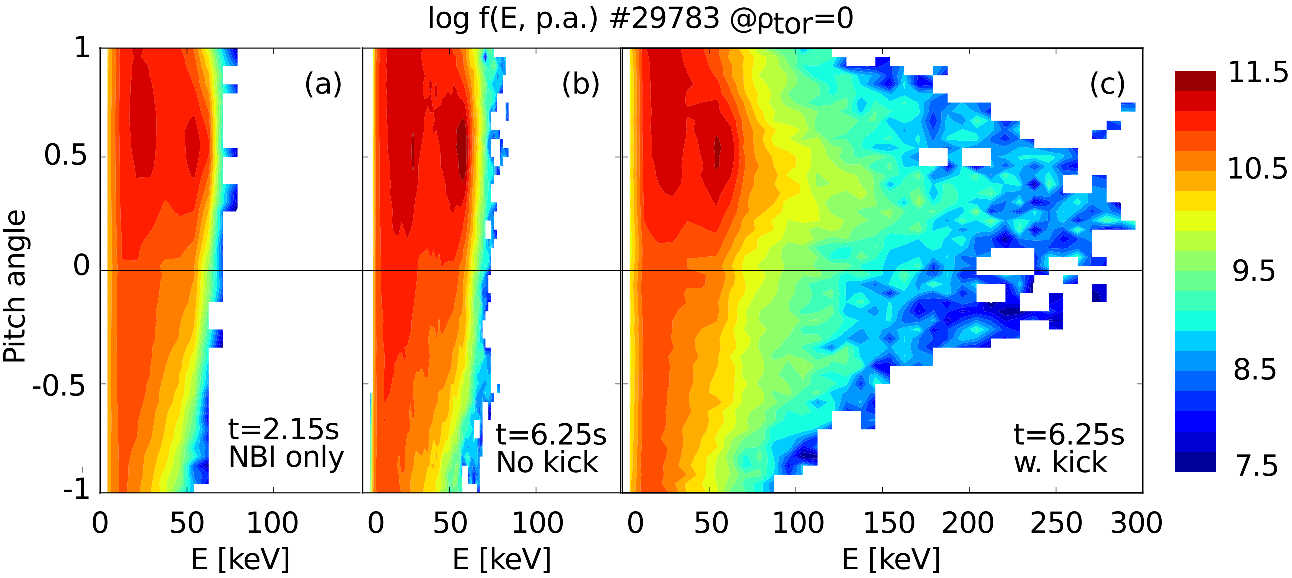

Figure 5. Energy/pitch fast ion distribution in the plasma center from TRANSP simulations. In the NBI-phase (a); in the NBI-ICRF phase, simulation without (b) and with RF-kick (c).

is a few orders of magnitude lower than below 60 keV, such energetic ions contribute significantly to the plasma pressure and they are more likely to undergo fusion reactions, due to the energy-dependence of the d-d cross-sections. A quantitative comparison with the neutron rates and spectra in the diagnostic's cone-of-sight is now possible.

4.1. Neutron rate simulation

In Fig. 6 we compare modelling results with and without RF-kick with experimental measurements, focussing on the increase at ICRF onset time. The RF-kick operator is obviously necessary to reconcile the simulations with the experimental neutron rate. This is the case for all analysed discharges. We summarise such a ratio for several

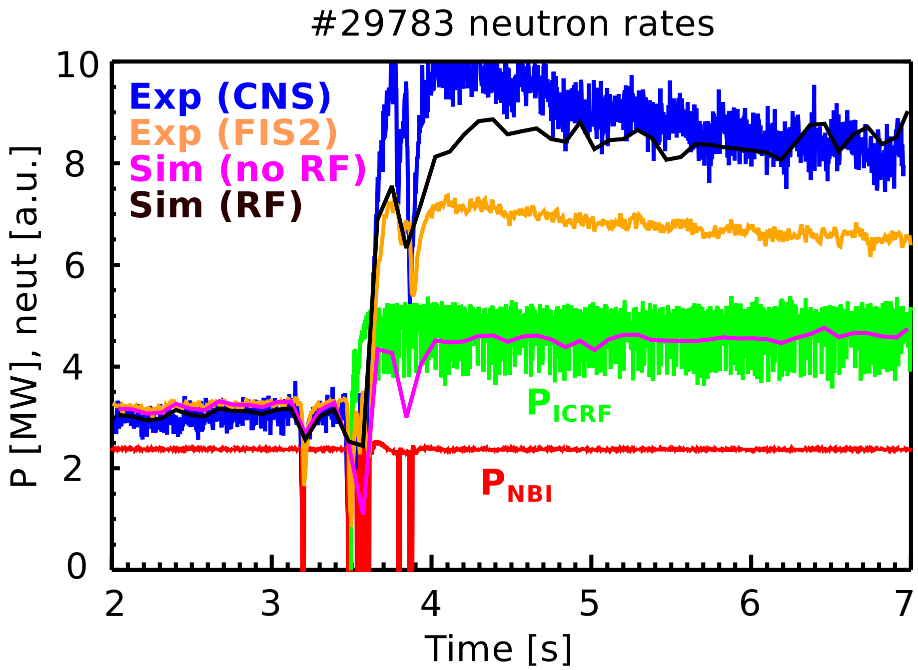

Figure 6. Measured and simulated neutron rates before and after switching on P_{ICRF} (green) on top of constant P_{NBI} (red): CNS (blue), FIS2 (orange), simulation with (black) and without RF-kick (magenta).

discharges and both diagnostics in Fig. 7. There is a considerable improvement in the agreement between measurement and simulation when including the RF-kick. The predicted ratio is accurate, in particular, when compared to the CNS measurement, which has a linear response over the whole relevant count rates' range - whereas FIS2 is not for rates above ∼3 10^{14} s^{-1}.

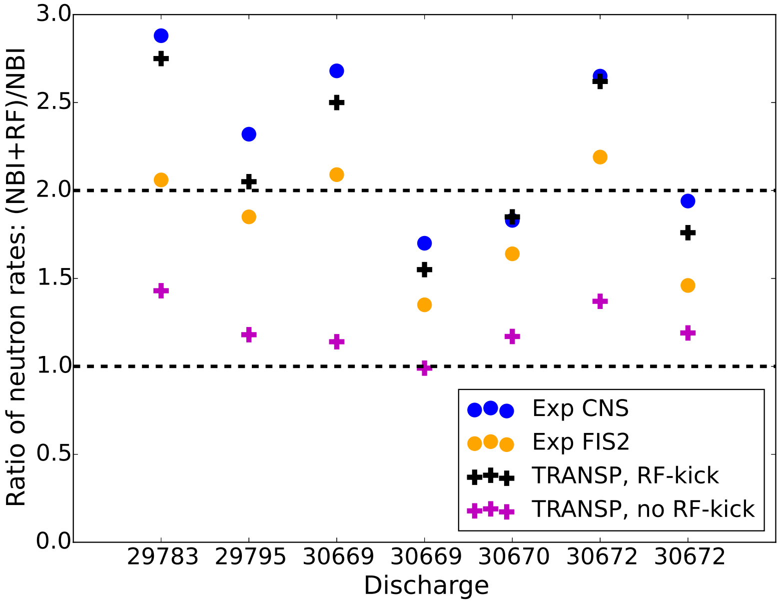

Figure 7. Measured and simulated ratio of neutron rates before and after switching on P_{ICRF} on top of constant P_{NBI}: CNS (blue), FIS2 (orange), TRANSP simulation with (black) and without RF-kick (magenta). Multiple time intervals are analysed for #30669 and #30672.

4.2. Neutron spectra

The GENESIS code [15] allows to calculate NES in the realistic cone-of-sight of the CNS, providing a fast ion distribution such as the one calculated by TRANSP/NUBEAM

(Fig. 5) or by TORIC+SSFPQL. The simulation result is shown in Fig. 8. The modification of the NES (Fig. 4), both in scale and in shape, can be compared with the deconvolution of the experimental PHS. The variation is well predicted in the case of TRANSP/NUBEAM (Fig. 8 (a)) whereas the energetic tail is largely overpredicted for TORIC+SSFPQL (Fig. 8 (b)). A possible explanation is the missing fast ion transport in TORIC+SSFPQL, which leads to a more effective acceleration of already accelerated fast ions and hence to an overestimate of the neutron rate and of the high-energy tail of the fast ion population and of the NES. The same trend is, of course, found also when convolving the simulated NES with the instrument response function, for comparison with the measured PHS of 3. Again, the TRANSP/NUBEAM package

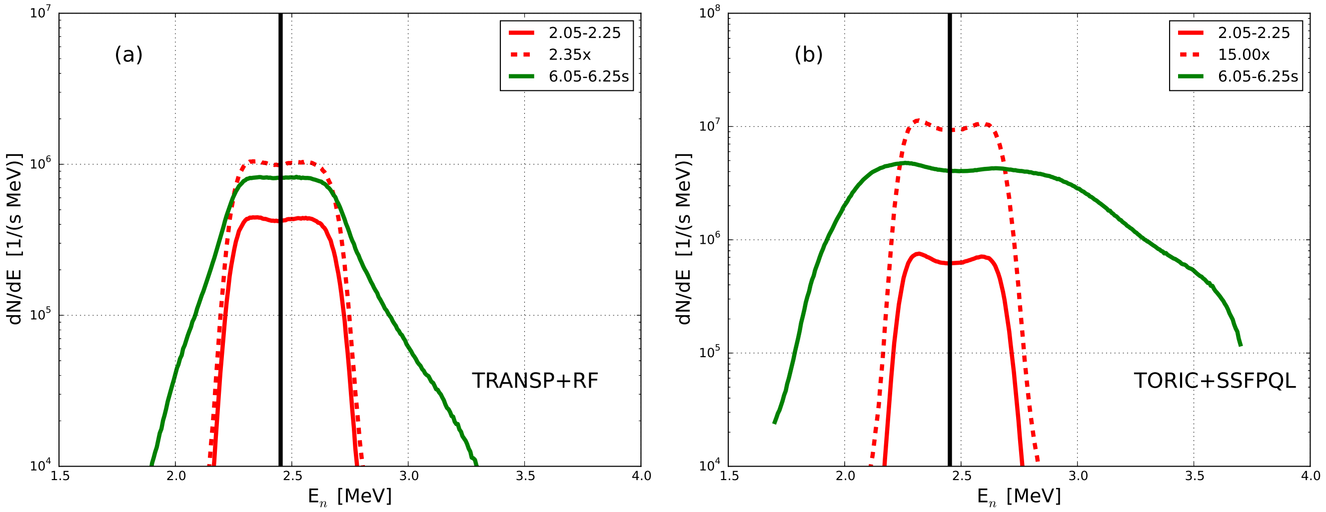

Figure 8. Semilogarithmic NES for discharge # 29783 calculated with GENESIS from plasma simulations with a) TRANSP+RF b) TORIC+SSFPQL. NBI phase (red continous), multiplied by a factor (red dashed) for comparison with NBI+ICRF (green).

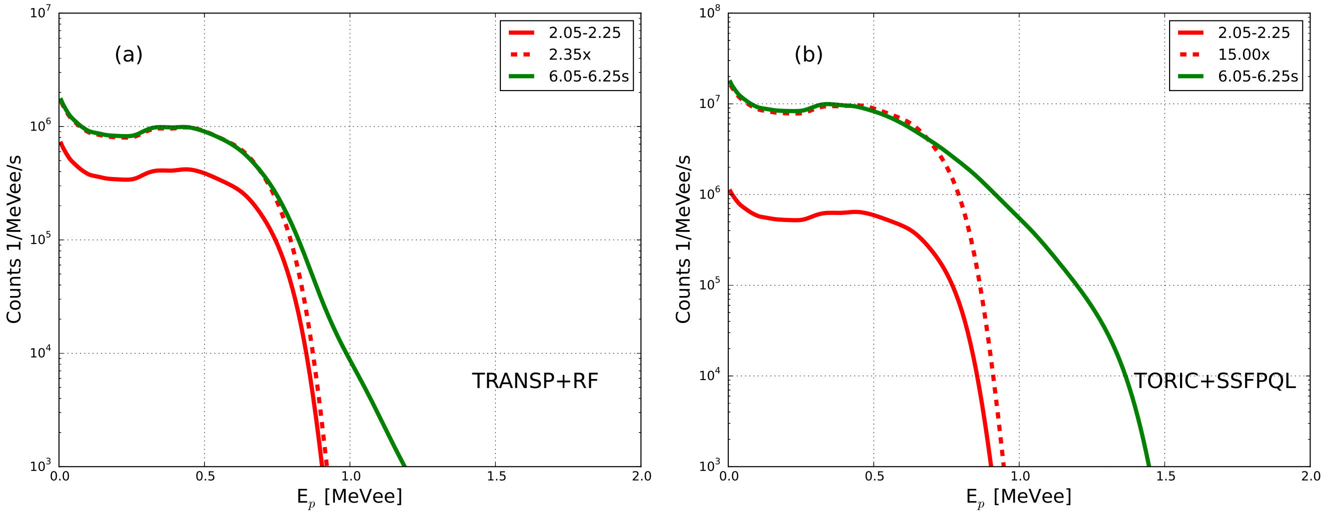

Figure 9. Semilogarithmic PHS for discharge # 29783 folding the GENESIS calculations with the instrumental response funnction. Plasma simulations with a) TRANSP+RF b) TORIC+SSFPQL. NBI phase (red continous), multiplied by a factor (red dashed) for comparison with NBI+ICRF (green).

with RF-kick gives an accurate prediction of the cheange in the PHS (Fig. 9 (a)), whereas TORIC+SSFPQL exhibits again a pronounced energetic tail (Fig. 9 (b)), consistently with Fig. 8.

4.3. Sensitivity study

A sensitivity study is performed, limiting the maximum energy of the TRANSP fast ion distribution. In Fig. 10 we plot the normalised NES and PHS corresponding to energy cuts at 60, 200 and 500 keV, as well as the cases without RF kick and with full distribution. The case with 60 keV is, as expected, overlapping the simulation without RF-kick. To give a deviation from the NBI-only case comparable with the experimental

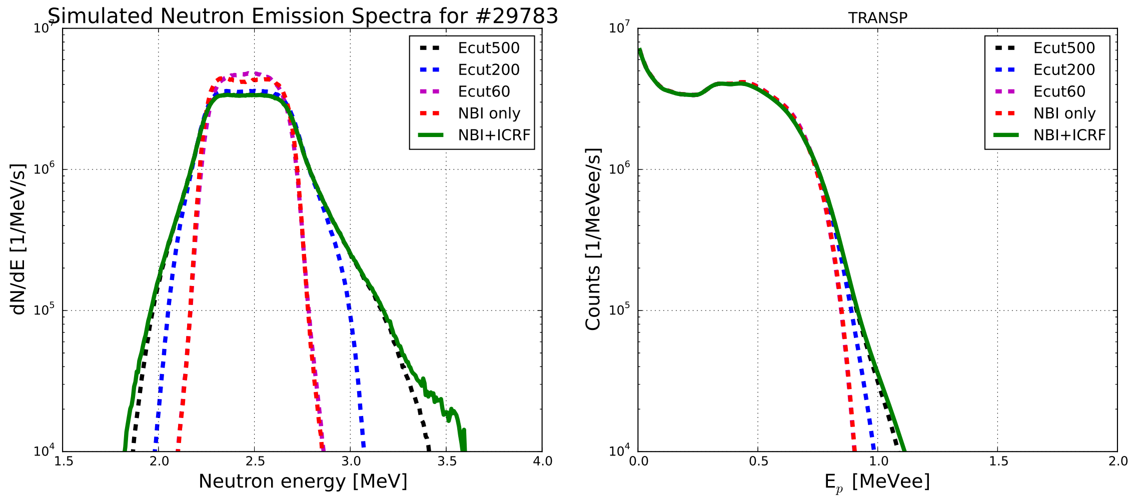

Figure 10. Sensitivity study for discharge # 29783 simulated with TRANSP+GENESIS cutting the fast ion energy

evidence (Figures 3 and 4) energies of the order of 500 keV appear to be necessary.

5. Conclusions

The well-known synergy effect between ICRF and NBI, yielding an anomalous increase of the neutron production, is shown to be a direct consequence of the acceleration of deuterium at 2nd harmonic. The measurements with the neutron spectrometer provides the experimental evidence for that, with a clear shape modification of the PHS towards energetic tails.

Modelling the effect by coupling plasma codes and neutron generation codes allows to assess quantitatively the effect: deuterium energies up to $\sim$ 500 keV are observed, one order of magnitude higher than the injection energy of the NBI. The deconvolution of the PHS into neutron emission spectra with two different unfolding methods (both based on entropy maximisation) confirms the fast ion energy around 500 keV, even though the spectra have uncertainties and a few artifacts.

The TRANSP simulation with RF-kick gives good quantitative prediction, suggesting that retaining fast ion transport is important to prevent an overestimate of the fast ion acceleration, which becomes more effective as the Larmor radius increases and can therefore easily amplify the effect.

Acknowledgement

This work has been carried out within the framework of the EUROfusion Consortium and has received funding from the Euratom research and training programme 2014-2018 under grant agreement No 633053. The views and opinions expressed herein do not necessarily reflect those of the European Commission.

[1] R. Bilato *et al* , Nuclear Fusion **51** (2011) 103034

[2] L.-G. Eriksson *et al* , Nuclear Fusion **38** (1998) 265-278

[3] M. Weiland *et al* , Nuclear Fusion **57** (2017) 116058

[4] G. Tardini *et al* , Journal of Instrumentation **7** (2012) C03004

[5] L. Giacomelli *et al* , Review of Scientific Instruments **82** (2011) 123504

[6] D. Marocco *et al* , IEEE Trans. Nucl. Sci. **56** (2009) 1168

[7] G. Tardini *et al* , Nuclear Fusion **53** (2013) 063027

[8] G. Tardini *et al* , Review of Scientific Instruments **87** (2016) 103504

[9] G. J. Wilkie *et al* , Plasma Phys. Control. Fusion **59** (2017) 044007

[10] M. Reginatto, A. Zimbal, Rev. Sci. Instruments **79** (2008) 023505

[11] R. Fischer *et al* , Proceedings of the Maximum Entropy Conference 1996, NMB Printers, Port Elizabeth, South Africa, 1997

[12] B. H. Park *et al* , Paper JP8.00122, Bull. Am. Phys. Soc. 54, (2012)

[13] A. Pankin, D. McCune, R. Andre *et al*, Comp. Phys. Comm. **159**, No. 3 (2004) 157

[14] M. Brambilla, Plasma Phys. Control. Fusion **41** (1999) 1-34

[15] M. Nocente *et al* , Nuclear Fusion **51** (2011) 063011